

High performance airbrushed organic thin film transistors

Calvin K. Chan,^{a)} Lee J. Richter, Brad Dinardo, Chernoy Jaye, Brad R. Conrad, Hyun Wook Ro, David S. Germack, Daniel A. Fischer, Dean M. DeLongchamp, and David J. Gundlach

National Institute of Standards and Technology, Gaithersburg, Maryland 20899-8120, USA

(Received 24 November 2009; accepted 8 February 2010; published online 30 March 2010)

Spray-deposited poly-3-hexylthiophene (P3HT) transistors were characterized using electrical and structural methods. Thin-film transistors with octyltrichlorosilane treated gate dielectrics and spray-deposited P3HT active layers exhibited a saturation regime mobility as high as $0.1 \text{ cm}^2 \text{ V}^{-1} \text{ s}^{-1}$, which is comparable to the best mobilities observed in high molecular mass P3HT transistors prepared using other methods. Optical and atomic force microscopy showed the presence of individual droplets with an average diameter of $20 \mu\text{m}$ and appreciable large-scale film inhomogeneities. Despite these inhomogeneities, near-edge x-ray absorption fine structure spectroscopy of the device-relevant channel interface indicated excellent orientation of the P3HT. © 2010 American Institute of Physics. [doi:10.1063/1.3360230]

Organic thin-film transistors (OTFTs) are promising for flexible, large area, and high volume applications such as display backplanes, sensor networks, and disposable electronics.¹⁻³ Although materials design and processing strategies have improved OTFT performance,⁴⁻⁶ development of inexpensive large-scale manufacturing methods remains a major barrier to commercialization. Fabrication processes using roll-to-roll (R2R) manufacturing offer a means of producing cheap organic electronics on flexible large-area substrates. While screen printing and doctor blading are currently the dominant techniques used in the R2R manufacturing of organic devices,⁷⁻¹⁰ spray deposition is receiving increased attention. Thin films are formed by depositing small aerosolized droplets, where fine control over the droplet size, solvent content, and solidification dynamics allows the formation of multilayer films while minimizing the dissolution of underlying layers. Although spray-deposited organic photovoltaic cells have been demonstrated with power conversion efficiencies comparable those of spin-cast cells,¹¹⁻¹³ very little work has been performed on spray-deposited OTFTs.

In this work, high-performance spray-deposited organic thin-film transistors with a poly-3-hexylthiophene (P3HT) active layer were investigated and compared with similar samples prepared using a spin coating process. The structural characteristics of airbrushed films were determined using ultraviolet-visible (UV-vis) absorption spectroscopy, optical microscopy (OM), atomic force microscopy (AFM), and near-edge x-ray absorption fine structure (NEXAFS) spectroscopy.

Spray-deposited P3HT films were fabricated using a commercially available airbrush kit [Iwata Kustom TH (Ref. 14)] with pressurized nitrogen as the carrier gas. Figure 1 illustrates the process scheme set up inside an ambient air fume hood with yellow filtered fluorescent lighting. High molecular mass P3HT (number average molecular mass $\approx 55 \text{ kg/mol}$, Plextronics Plexcore OS 2100) was used for these experiments, while substrates consisting of quartz,

thermally grown SiO_2 , and thin-film transistor structures were selected as appropriate for each characterization method. All substrates were pretreated with octyltrichlorosilane (OTS8, Sigma-Aldrich) using an established solution process.¹⁵ Samples were placed on a $85 \text{ }^\circ\text{C}$ hotplate while a solution of 2 mg/mL P3HT dissolved in 6:1 chlorobenzene:1,2,3,4-tetrahydronaphthalene was sprayed onto the substrates. Critical parameters used in the spray procedure included the carrier gas pressure (172 kPa), draw rate (10 cm/s), flow rate ($40 \mu\text{L/s}$), and throw distance (18 cm). Twenty coats of P3HT were applied to the substrates with a 10 s pause in between every other coat. P3HT films were also prepared by spin coating at 500 rpm for 3 min inside an Ar glovebox using the same P3HT solution. The spin-coated films were then exposed to the same postdeposition conditions (30 min , $85 \text{ }^\circ\text{C}$, in air) as the spray-coated films.

The thickness of a spun cast P3HT film on OTS8/SiO_2 was $\approx 12 \text{ nm}$ as measured using spectroscopic ellipsometry. The thickness of spray-deposited P3HT films could not be determined with ellipsometric measurements due to difficulties in obtaining a specular reflection from their rough surfaces. Optical and AFM images of spray-deposited P3HT films are shown in Figs. 2(a) and 2(b), respectively, confirm-

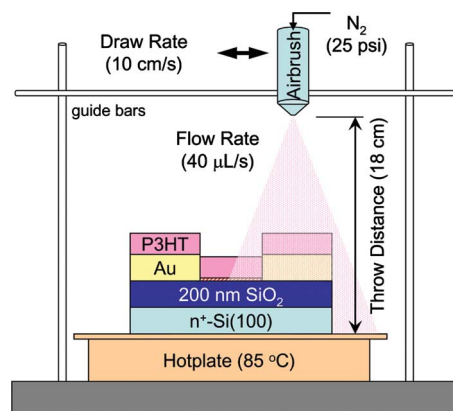


FIG. 1. (Color online) Schematic drawing of the spray deposition setup showing the relevant processing parameters used for the fabrication of P3HT films. Also shown is the OTFT device structure used for electrical characterization.

^{a)} Author to whom correspondence should be addressed. Electronic mail: calvin.chan@nist.gov.

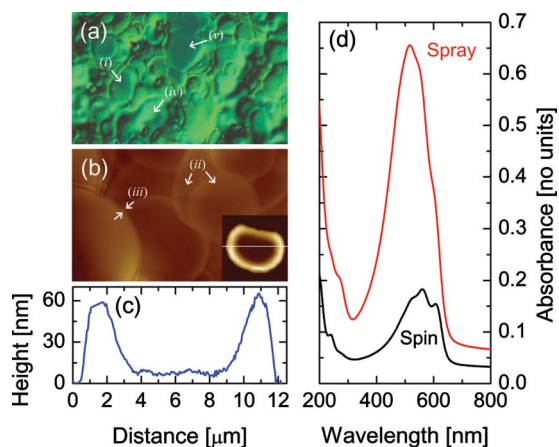


FIG. 2. (Color online) (a) Optical microscopy ($150\ \mu\text{m} \times 250\ \mu\text{m}$) and (b) AFM ($30\ \mu\text{m} \times 50\ \mu\text{m}$) images taken from the top surface of spray-deposited P3HT films. The AFM height contrast is 250 nm. Various features are indicated by the arrows. A single solidified P3HT droplet on flat OTS8/SiO₂ is shown inset in (b), where (c) is a line scan across the droplet. (d) UV-vis absorption spectra for P3HT films spray and spin deposited onto OTS8/quartz substrates.

ing the rough top surface of airbrushed films. The images exhibit round features corresponding to droplets with an average diameter of $20\ \mu\text{m}$. Other observed structural features include (i) merging of droplets, (ii) superposition of droplets, (iii) coffee stain effects, (iv) spherical solidification, and (v) planar film formation. The inset in Fig. 2(b) shows an image of a single P3HT droplet on a flat OTS8/SiO₂ substrate, and further highlights the dominant film structure. A line scan through the center of the droplet [Fig. 2(c)] shows a very flat interior region with an average thickness of 7 nm. The droplet is surrounded by a sharp outer ring nearly 60 nm thick. These effects lead to the formation of an inhomogeneous film with large-scale surface roughness measurable by the high root mean square (rms) roughness of ≈ 100 nm. Despite the overall irregularity of the spray-deposited film, the center region within each droplet was very smooth, exhibiting typical rms roughnesses of < 20 nm.

Optical absorption was used to estimate the average thickness of spray-deposited films. The UV-vis absorption spectra for P3HT films spray- and spin-deposited onto OTS8/quartz substrates is plotted in Fig. 2(d). Comparing the area under the P3HT absorption region (315–750 nm), and assuming a Lambert–Beer relationship, the spray-deposited film was estimated to be ≈ 100 nm thick on average. The relative magnitude of the 0–0 and 0–1 vibronic features can be related to the exciton bandwidth and intrachain order.^{16,17} Spectra with strong 0–0 features as seen in the spin-cast film are reflective of high degrees of order. On the other hand, the vibronic structure in the spray-coated film is clearly less pronounced (weak 0–0 transition). While quantitative analysis is precluded due to the significant variations in films thickness, the bulk of the spray films appear significantly less ordered.

To investigate the effects of film homogeneity and local order on the performance of spray-deposited P3HT OTFTs, films were sprayed onto transistor structures consisting of a n⁺-Si(100) gate electrode, a 200 nm OTS8/SiO₂ gate dielectric, and photolithographically patterned 1 nm Ti/20 nm Au source-drain contacts. Spin-deposited P3HT transistors were also fabricated for comparison. Channel lengths included 10, 20, 25, 50, 80, and $100\ \mu\text{m}$, while the width was fixed at

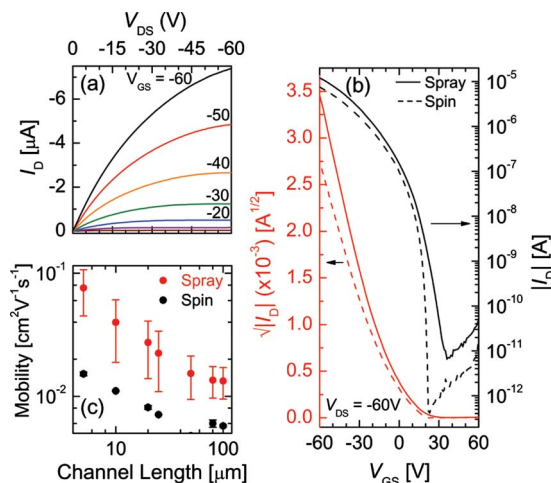


FIG. 3. (Color online) (a) (I_D - V_{DS}) curves as a function of gate bias ($V_{GS}=0$ to -60 V) for a typical spray-coated P3HT thin-film transistor. (b) Saturation regime transfer curves (I_D - V_{GS} for $V_{DS}=-60$ V) for spray- and spin-deposited P3HT transistors. Both sets of measurements were obtained from transistors with L/W ratios of $1000/25\ \mu\text{m}/\ \mu\text{m}$. (c) The average and standard deviation of saturation regime mobilities for spray- and spin-deposited films plotted as a function of channel length.

$1000\ \mu\text{m}$. All electrical characterization was conducted in an Ar environment. Figure 3(a) shows a representative set of current-voltage (I_D - V_{DS}) curves as a function of gate voltage (V_{GS}) for a spray-deposited P3HT transistor with a channel length of $25\ \mu\text{m}$ as measured in an inert environment. Figure 3(b) plots typical saturation regime current-voltage (I_D - V_{GS}) curves for the same device, as well as a device fabricated using spin casting. Table I summarizes the ensemble performance metrics for a large number (50+) of spray- and spin-deposited P3HT OTFTs, including the average and standard deviation of the saturation regime mobilities (μ_{avg}), the range of subthreshold slopes (S_{th}) and threshold voltages (V_{th}), and typical on/off current ratios ($I_{\text{on}}/I_{\text{off}}$). Annealing of the transistors at $85\ ^\circ\text{C}$ in a vacuum oven for 12 h produced no noticeable improvements in device performance, although improvements in S_{th} , V_{th} , and $I_{\text{on}}/I_{\text{off}}$ are expected for devices processed under inert conditions. The saturation regime field-effect mobility observed in spin-cast P3HT films was $0.009 \pm 0.004\ \text{cm}^2\ \text{V}^{-1}\ \text{s}^{-1}$, which is typical for high molecular weight P3HT OTFTs,¹⁷ whereas spray-deposited P3HT transistors exhibited a higher average mobility of $0.023 \pm 0.016\ \text{cm}^2\ \text{V}^{-1}\ \text{s}^{-1}$. The increased variability in the spray-deposited film may reflect both its increased film inhomogeneity and its ambient processing conditions. The channel length dependence of the saturation regime mobilities for spray- and spin-coated films is shown in Fig. 3(c). Both devices exhibit increasing mobility as a function of

TABLE I. Summary of the performance metrics obtained from a large set of spray- and spin-deposited P3HT thin-film transistors. The dichroic ratios (R) determined using NEXAFS are also listed.

	μ_{avg} ($\text{cm}^2/\text{V/s}$)	S_{th} (V/dec)	V_{th} (V)	$I_{\text{on}}/I_{\text{off}}$	R_{bot}
Spray	0.023 ± 0.016	3.0–6.0	10–20	10^6	0.21
Spin	0.009 ± 0.004	0.6–1.8	15–30	10^7	0.22
Spray annealed	0.020 ± 0.013	2.5–4.0	10–20	10^7	0.25
Spin annealed	0.008 ± 0.003	0.4–1.2	15–30	10^7	0.21

decreasing channel length, which is in contrast to what is typically observed for contact-limited devices. One might attribute this to either a field-enhanced charge transport mechanism or charge transport that is limited by the structural imperfections such as grain boundaries.^{18–20} In the latter case, it is possible that as the channel decreases below the droplet size ($\sim 25\text{--}50\ \mu\text{m}$), mobility increases due to the presence of fewer droplet boundaries in the transport pathway. Nevertheless, relatively high-performance airbrushed P3HT transistors have been demonstrated despite the presence of these significant surface heterogeneities and poor bulk order.

The molecular orientation of P3HT at the dielectric interface is an important factor affecting charge transport in OTFT channels. This orientation was measured using NEXAFS spectroscopy to determine whether it could explain the surprisingly comparable device performance between spray- and spin-deposited P3HT transistors. The angle-dependent intensity of the carbon K-edge $1s \rightarrow \pi^*$ transition in P3HT provides information about the orientation of its transport-relevant π -conjugated backbone plane, where the dichroic ratio (R) is a quantitative metric of this orientation.²¹ The value of R varies between -1 and 0.7 depending on whether the π orbitals of the P3HT backbone are oriented on average perpendicular or parallel to the surface, respectively. In order to determine the average polymer orientation at the gate interface, spin- and spray-deposited P3HT films were delaminated from the OTS8/SiO₂ substrate using parylene as the top adhesive. NEXAFS on the delaminated OTS8/SiO₂ surface exhibited no residual P3HT features, indicating full removal of the polymer film. As tabulated in Table I, the dichroic ratios for bottom P3HT interfaces show equivalent values of $R_{\text{bot}} \approx 0.21$ and $R_{\text{bot}} \approx 0.22$ for the spray- and spin-deposited films, respectively. This suggests that the transport-relevant molecular orientation at the organic-dielectric interface is similar for both spin- and spray-deposited P3HT. Not only are these values consistent with those reported in literature²¹ but they may also explain why spin- and spray-deposited P3HT transistors perform comparably well.

In summary, thin-film transistors fabricated using a facile airbrush deposition technique were shown to have high performance comparable to standard spin-coated equivalents. Although OM and AFM indicate the presence of microscale film inhomogeneities, and UV-vis absorption spectroscopy indicates significant bulk conformational disorder, NEXAFS spectroscopy suggests that P3HT at the dielectric interface

has a molecular orientation consistent with good π overlap in the OTFT source-drain plane.

Financial support from the NIST/NRC Postdoctoral Association for C.K.C. and B.R.C. is gratefully acknowledged.

- ¹G. H. Gelinck, H. E. A. Huitema, E. V. Veenendaal, E. Cantatore, L. Schrijnemakers, J. B. P. H. van der Putten, T. C. T. Geuns, M. Beenhakkers, J. B. Giesbers, B.-H. Huisman, E. J. Meijer, E. M. Benito, F. J. Touwslager, A. W. Marsman, B. J. E. van Rens, and D. M. de Leeuw, *Nature Mater.* **3**, 106 (2004).
- ²T. Someya, B. Pal, J. Huang, and H. E. Katz, *MRS Bull.* **33**, 690 (2008).
- ³P. F. Baude, D. A. Ender, M. A. Haase, T. W. Kelley, D. V. Muires, and S. D. Theiss, *Appl. Phys. Lett.* **82**, 3964 (2003).
- ⁴J. E. Anthony, *Chem. Rev.* **106**, 5028 (2006).
- ⁵D. Shukla, S. F. Nelson, D. C. Freeman, M. Rajeswaran, W. G. Ahearn, D. M. Meyer, and J. T. Carey, *Chem. Mater.* **20**, 7486 (2008).
- ⁶D. J. Gundlach, J. E. Royer, S. K. Park, S. Subramanian, O. D. Jurchescu, B. H. Hamadani, A. J. Moad, R. J. Kline, C. L. Teague, O. Kirillov, C. A. Richter, J. G. Kushmerick, L. J. Richter, S. R. Parkin, T. N. Jackson, and J. E. Anthony, *Nature Mater.* **7**, 216 (2008).
- ⁷S. Holdcroft, *Adv. Mater.* **13**, 1753 (2001).
- ⁸S. E. Shaheen, R. Radspinner, N. Peyghambarian, and G. E. Jabbour, *Appl. Phys. Lett.* **79**, 2996 (2001).
- ⁹A. C. Huebler, F. Doetz, H. Kempa, H. E. Katz, M. Bartzsch, N. Brandt, I. Hennig, U. Fuegmann, S. Vaidyanathan, J. Granstrom, S. Liu, A. Sydorenko, T. Zillger, G. Schmidt, K. Preissler, E. Reichmanis, P. Eckerle, F. Richter, T. Fischer, and U. Hahn, *Org. Electron.* **8**, 480 (2007).
- ¹⁰C. J. Brabec and J. R. Durrant, *MRS Bull.* **33**, 670 (2008).
- ¹¹R. Green, A. Morfa, A. J. Ferguson, N. Kopidakis, G. Rumbles, and S. E. Shaheen, *Appl. Phys. Lett.* **92**, 033301 (2008).
- ¹²S. F. Tedde, J. Kern, T. Sterzl, J. Fürst, P. Lugli, and O. Hayden, *Nano Lett.* **9**, 980 (2009).
- ¹³C. N. Hoth, R. Steim, P. Schilinsky, S. A. Choulis, S. F. Tedde, O. Hayden, and C. J. Brabec, *Org. Electron.* **10**, 587 (2009).
- ¹⁴Any mention of commercial products is for information only; it does not imply recommendation or endorsement by NIST.
- ¹⁵R. J. Kline, D. M. DeLongchamp, D. A. Fischer, E. K. Lin, M. Heeney, I. McCulloch, and M. F. Toney, *Appl. Phys. Lett.* **90**, 062117 (2007).
- ¹⁶J. Clark, J.-F. Chang, F. C. Spano, R. H. Friend, and C. Silva, *Appl. Phys. Lett.* **94**, 163306 (2009).
- ¹⁷J.-F. Chang, J. Clark, N. Zhao, H. Sirringhaus, D. W. Breiby, J. W. Andreasen, M. M. Nielsen, M. Giles, M. Heeney, and I. McCulloch, *Phys. Rev. B* **74**, 115318 (2006).
- ¹⁸B. H. Hamadani, D. J. Gundlach, I. McCulloch, and M. Heeney, *Appl. Phys. Lett.* **91**, 243512 (2007).
- ¹⁹B. H. Hamadani, J. L. LeBoeuf, R. J. Kline, I. McCulloch, M. Heeney, C. A. Richter, L. J. Richter, and D. J. Gundlach, *Proc. SPIE* **6658**, 66580V (2007).
- ²⁰L. H. Jimison, M. F. Toney, I. McCulloch, M. Heeney, and A. Salleo, *Adv. Mater.* **21**, 1568 (2009).
- ²¹D. M. DeLongchamp, E. K. Lin, and D. A. Fischer, in *Organic Field Effect Transistors*, edited by Z. Bao and J. Locklin (CRC/Taylor & Francis, Boca Raton, FL, 2007), pp. 277–296.